



Article

Influence of Moisture Content on Some Mechanical Properties of Wheat

Manuel Moya ^{1,*} , David Sánchez ², José Ángel Romero ² and José Ramón Villar-García ¹ 

¹ Forest Research Group, Department of Forestry and Agricultural Medium Engineering, University Center of Plasencia, University of Extremadura, Avda. Virgen del Puerto n° 2, 10600 Plasencia (Cáceres), Spain; jrvillar@unex.es

² University Center of Plasencia, University of Extremadura, Avda. Virgen del Puerto n° 2, 10600 Plasencia (Cáceres), Spain; davidsavi4jaraiz@gmail.com (D.S.); romerolopezjangel@gmail.com (J.Á.R.)

* Correspondence: manuelmi@unex.es

Abstract: The loads generated inside agricultural silos under static and dynamic conditions depend on the mechanical properties of the materials stored inside them. Silo calculation methodologies are based on these mechanical properties. Although it is known that moisture content greatly influences the values reached by these mechanical properties, only a few studies have been conducted to determine them. The present work determines the angle of internal friction, the apparent cohesion, the dilatancy angle and the apparent specific weight of wheat when subjected to different moisture contents. Direct shear and oedometer assay devices were used. In addition, a climatic chamber was used to moisten the wheat samples used in this work. From the different assays conducted, it could be observed that the values of the angle of internal friction, the apparent cohesion and the apparent specific weight were like those found in the literature. However, no values of the dilatancy angle of wheat as influenced by moisture content were previously reported. The values obtained here for this parameter are within the range of those specified for dry wheat samples. Finally, higher apparent specific weight values were observed as moisture content increased up to 13.4%, then decreasing at a moisture content of 15.5%. This was not expected according to the results stated by some authors, although others reported a similar tendency. The values here provided can be used in silo load calculations involving numerical methods for modeling technological processes.

Keywords: agricultural silos; numerical methods; mechanical properties; wheat; angle of internal friction; specific weight; apparent cohesion; moisture content



Citation: Moya, M.; Sánchez, D.; Romero, J.Á.; Villar-García, J.R. Influence of Moisture Content on Some Mechanical Properties of Wheat. *Agronomy* **2024**, *14*, 347. <https://doi.org/10.3390/agronomy14020347>

Academic Editor: Yanbo Huang

Received: 12 January 2024

Revised: 2 February 2024

Accepted: 6 February 2024

Published: 8 February 2024



Copyright: © 2024 by the authors. Licensee MDPI, Basel, Switzerland. This article is an open access article distributed under the terms and conditions of the Creative Commons Attribution (CC BY) license (<https://creativecommons.org/licenses/by/4.0/>).

1. Introduction

The loads generated inside agricultural silos can be calculated using both classical and numerical methodologies. Classical theories are suitable for determining these loads under static conditions, with the Janssen formula [1] being the world's most widely used. However, numerical methods began to be applied to silo calculations in the 1970s [2], and since then, they have experienced a great surge, especially during the 21st century, thanks to advances in computing [3–12]. With these techniques, it is possible to accurately predict dynamic loads occurring during both the filling and the emptying of silos, in addition to modeling the static conditions. In any case, with all of these methodologies, it is necessary to consider different mechanical properties of the materials stored inside agricultural silos, such as the angle of internal friction, the apparent cohesion, the friction coefficient, the bulk density or the Young's modulus, among others. Values and studies of these parameters can be found within the literature for both granular and powdered materials [13–26]. These data refer to dry samples, i.e., materials with an ambient humidity. Nevertheless, it has been well known for a long time that these material properties, the loads as well as the type of flow that they generate inside silos, are greatly influenced by moisture content, as shown in some works [13,27–37].

Notwithstanding the above, to date, there are not many works reported in the literature focused on the study of the influence of humidity when intermediate liquid contents are considered. They mainly refer to the pendular state but rarely to the funicular state [38–40]. Under humidity effects, capillary forces appear when water molecules are placed between the grains. Under these circumstances, both the cohesion and the friction of the material are affected [32,41,42]. The amount of liquid present in the granular medium allows for the establishment of capillary bridges between the grains, and it determines the pendular, funicular or capillary states. These liquid bridges and/or capillary bridges can be created or destroyed as a material passes from a dry state to a wet one, or vice versa. This affects the shear strength, the friction between particles, the lubricating role of water or the cohesive behavior of the material, among other factors [40,43–48].

The aim of the present work was to provide values of the following mechanical properties: the angle of internal friction, the apparent cohesion, the apparent specific weight and the dilatancy angle. The material tested was wheat (*Triticum*) subjected to different moisture contents. The results add to those already reported in the literature for the first three and provide the first information of this kind for the fourth. In addition, these values could be useful for studying the mechanical behavior of wheat when its moisture content is varied.

2. Materials and Methods

The assays conducted were all performed at the Geotechnical Laboratory of the Centro Universitario de Plasencia (University of Extremadura). The material used in this work was wheat (Leonesa Astur de Piensos, S.A. (LESA), León, Spain).

The properties determined for this material were as follows: the angle of internal friction (ϕ), the apparent cohesion (C), the dilatancy angle (ψ) and the apparent specific weight (γ).

A description of the different assays carried out to determine the values of these parameters has been provided in detail elsewhere [21,22]. However, information regarding particular conditions is provided below.

2.1. Climatic Chamber

Wheat samples were subjected to different moisture contents and temperatures by means of a climatic chamber available at the laboratory. A touch screen placed at the upper right side of the device allowed us to select different values for the temperature and the relative humidity within the device. The range of temperatures ranged from +5 °C to 60 °C, whereas the relative humidity ranged from 15% to 95%. For the temperature, the stability ranged from ± 0.2 to ± 2 °C, whereas the uniformity ranged from $\pm 1\%$ to $\pm 5\%$. In the case of the relative humidity, the stability ranged from $\pm 1\%$ to $\pm 5\%$, whereas the uniformity ranged from $\pm 1\%$ to $\pm 5\%$. In this work, five different combinations of temperature and relative humidity were established for the wheat sample placed within it. The minimum temperature selected was 20 °C. For this temperature, relative humidities of 35, 45, 65 and 90% were selected, whereas for the highest temperature tested (55 °C), a relative humidity of 25% was chosen. Wheat samples were subjected to each of these combinations of temperature and relative humidity for a minimum of 72 h to achieve homogeneity of moisture content in the samples used before beginning the corresponding assays. Figure 1 shows the climatic chamber used in this work (Figure 1a) and the touch screen for selecting the temperature and the relative humidity (Figure 1b).

2.2. Determination of the Moisture Content

Wheat samples were dried in an oven at 105–110 °C, adhering to Part 1 of Standard UNE-EN ISO 17892 [49]. Each of them was weighed every 24 h until a constant weight was reached. An electronic balance with a precision of 0.01 kg was used. Figure 2 shows the electronic balances used for determining the moisture content of the samples (right) and the weight of the oedometric cell (left). This last one had a precision of 0.1 kg.



Figure 1. Climatic chamber device (a) and the screen for selecting the temperature and the relative humidity (b).



Figure 2. Electronic balances used in this work.

2.3. Direct Shear Assays

The assays conducted in this work adhered to the procedure established in Part 10 of Standard UNE-EN ISO 17892 [50]. The parameters determined with this device were the angle of internal friction, the apparent cohesion and the dilatancy angle. The main characteristics of the semi-automatic direct shear test device were reported in an earlier work [23]. The stress was established by means of a 10:1 dead-weight beam loading system, which allowed us to apply vertical confining pressures, as depicted in Figure 3a. In addition, a touch screen, which can be observed at the right side of the direct shear device in Figure 3a and is more detailed in Figure 3b, allowed us to set the speed selected for the assays. The strain rate was precisely controlled from 0.00001 to 10 mm/min by an advanced stepper motor drive system. The maximum shear displacement was 20 mm. The shear strength of the sample was recorded by means of a load cell, whereas the vertical deformation and the horizontal displacement were recorded with the help of two strain gauge transducers with 100 mm travel. The data obtained from these assays (shear stress, vertical strain and horizontal displacement) were collected with the help of software provided with the direct shear device. This software allowed us to export them as “.xls” files and thus, using an Excel spreadsheet for Microsoft 365, the different graphs and tables shown in Section 3

could be obtained. In this research work, the normal stresses applied to the wheat samples were 10, 20, 50, 100, 200 and 300 kPa. The assay speed was 0.4 mm/min. This speed was high enough to prevent the sample from losing humidity while the test was performed. The assay was replicated twice at each stress level. Figure 3 shows the direct shear device used (Figure 3a) and the touch screen for selecting the speed of the assays conducted (Figure 3b):



(a)



(b)

Figure 3. Direct shear device (a) and the touch screen (b) for selecting the speed of the assays conducted.

2.4. Oedometric Assays

The oedometric assays were performed according to the procedure described in Part 5 of Standard UNE-EN ISO 17892 [51]. The parameter determined with this device was the apparent specific weight of the material. The main characteristics of this device were also provided in an earlier work [23]. The assay modality carried out on this occasion was the abbreviated one. It consisted of conducting an automatic increase or a decrease in the load applied just when a maximum deformation of 0.1 mm was reached for three consecutive hours. In that case, primary consolidation is assumed to have occurred. Faster assays could be conducted this way compared to the traditional ones, considering that the samples had specific humidity conditions. Normal stresses of 8, 16, 32, 64, 128 and 256 kPa were applied. All assays were performed in triplicate.

The apparent specific weight of the material could be obtained as follows: The amount of sample placed within the oedometric cell was weighed right before beginning the assay. As the cells used in these assays are standardized (75 mm in diameter and 20 mm in height), their volume is known. Initially, the wheat sample occupied the entire volume of the oedometric cell (V). Once the assay started, the normal pressure exerted on the cell (P) compressed the grain sample, thus reducing the height that it occupied inside (H'). Once the maximum vertical stress was applied to the sample, the loading cycle was finished and the wheat sample occupied the minimum volume (V'), thus reaching its maximum apparent specific weight. Then, the unloading cycle began, and as the vertical load was progressively reduced, the material was less compressed, and the height occupied inside the cell increased. The height of the sample within the corresponding oedometric cell could be measured every time with the help of a displacement transducer. This way, the volume occupied by the sample after each loading step could be calculated and so the apparent specific weight of the material could be determined. Figure 4 shows the procedure described:

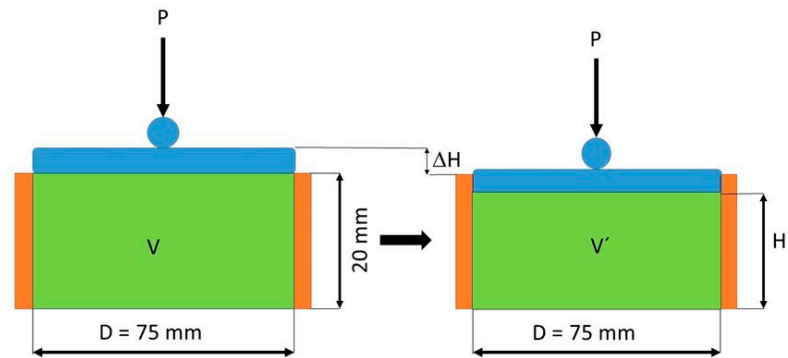


Figure 4. Scheme of the oedometric assay conducted to determine the apparent specific weight.

The data obtained from these assays (confining pressure and vertical strain) were collected with the help of software provided with the automatic oedometric device. As explained for direct shear assays, files generated with this software were inputted to an Excel spreadsheet for Microsoft 365, thus obtaining the graphs and tables shown in the Section 3.

3. Results

3.1. Moisture Content

Wheat samples were subjected to different combinations of temperature and relative humidity within the climatic chamber. A small amount of the wheat sample was chosen to determine its moisture content prior to beginning the assays. The moisture content of the sample was determined by drying it in the oven, as described in the previous section. Thus, the real moisture content of the sample could be determined. Table 1 shows the different combinations of temperature and relative humidity and their corresponding real moisture content expressed on a dry basis (d.b.).

Table 1. Combinations of temperature and relative humidity used in this work and their corresponding real moisture content (d.b.) determined by drying the samples in an oven at 105–110 °C.

Climatic Chamber Conditions		Moisture Content (d.b.) (%)
Temperature (°C)	Relative Humidity (%)	
55	25	7.5
20	35	10
20	45	10.5
20	65	13.4
20	90	15.5

From the previous table, it can be seen that the moisture content of wheat samples ranged from 7.5 to 15.5%. This range of values is within that reported in other works [13,31,52].

3.2. Direct Shear Assays

3.2.1. Angle of Internal Friction and Apparent Cohesion

Stress–strain curves showing the relationship between the shear stress and the horizontal displacement at six different normal stresses (10, 20, 50, 100, 200 and 300 kPa) are plotted for the two replications carried out at moisture contents of 15.5% (Figure 5) and 7.5% d.b. (Figure 6), respectively:

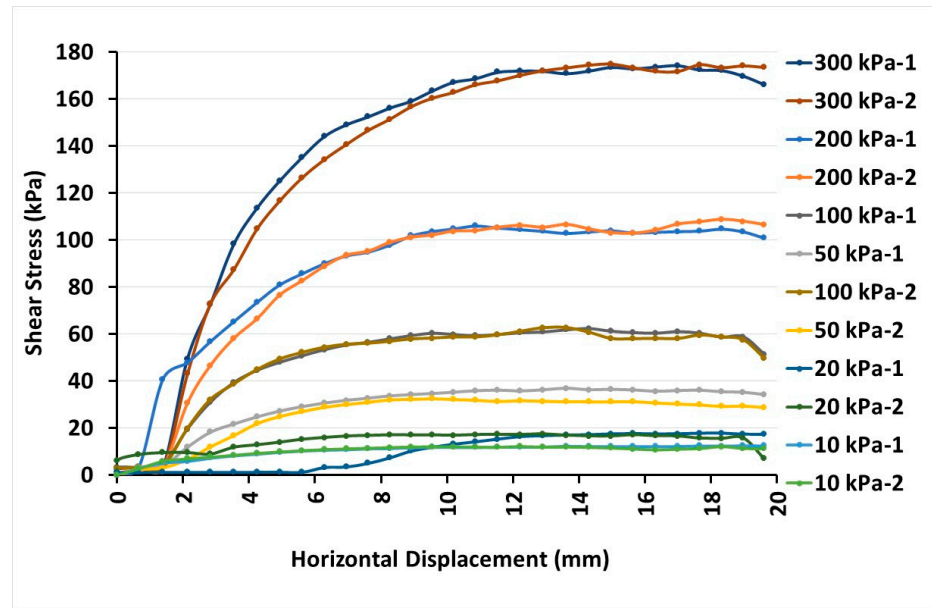


Figure 5. Stress–strain curves obtained for wheat samples at normal stresses of 10, 20, 50, 100, 200 and 300 kPa for the two replications conducted at moisture content of 15.5% d.b.

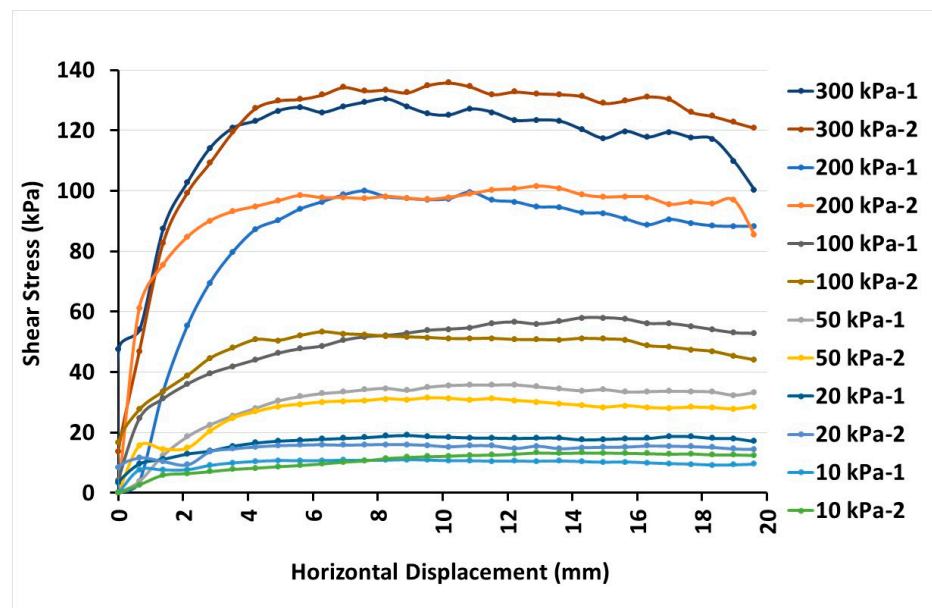


Figure 6. Stress–strain curves obtained for wheat samples at normal stresses of 10, 20, 50, 100, 200 and 300 kPa for the two replications conducted at moisture content of 7.5% d.b.

As expected, the higher the normal stress applied, the higher the shear stress reached. The peak value obtained for the lateral stress at a normal stress of 300 kPa and a moisture content of 15.5% was 175 kPa, which was a 29% higher than that reached when a moisture content of 7.5% was applied (136 kPa). However, lower differences (6.8 and 8.6%, respectively) were observed when normal stresses of 200 and 100 kPa were applied at both moisture contents. It should be noted that in this case, at lower applied normal stresses (10, 20 and 50 kPa), the highest value obtained for the shear stress was higher at a lower moisture content. This difference was 2.7%, 5.6% and 8.1% at 50, 20 and 10 kPa, respectively. Nevertheless, this trend could not be confirmed at intermediate moisture contents (10, 10.5 and 13.4%, respectively), where at lower normal stresses, the lateral stress was higher as

moisture content increased. Finally, the shape of the curves was similar to those shown in Figure 4 for the samples assayed at moisture contents of 10, 10.5 and 13.4%, respectively.

The regression lines for the Mohr–Coulomb strength envelopes obtained in the assays conducted at the different normal stresses and moisture contents considered are shown in Figure 7. The slope of these lines provides the value of the angle of internal friction, whereas the intersection with the ordinate axis provides that of the apparent cohesion.

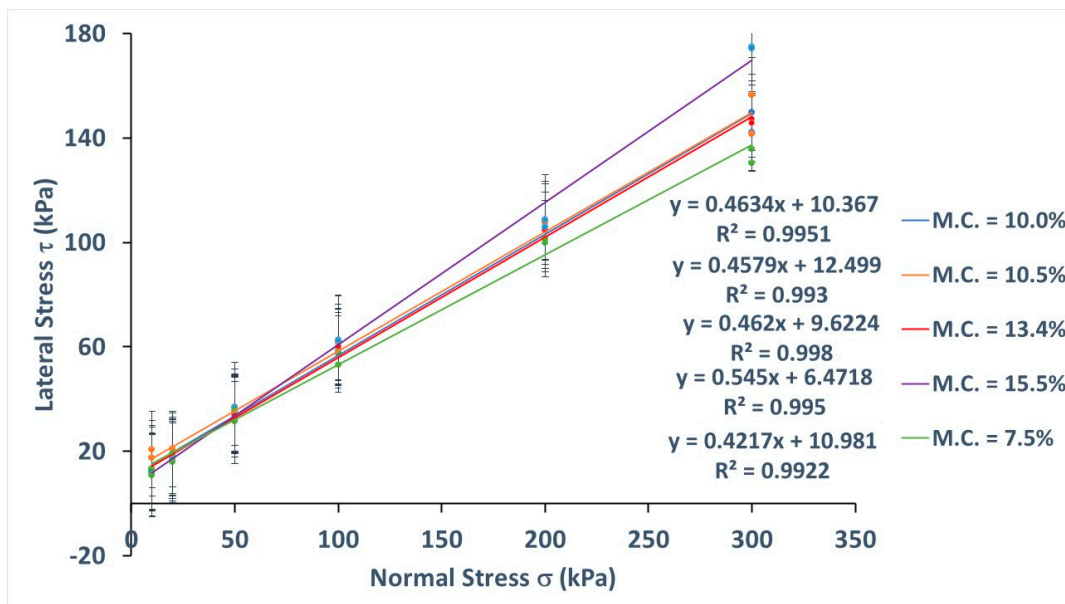


Figure 7. Regression lines for the Mohr–Coulomb strength envelopes obtained from direct shear assays conducted at different moisture contents.

As it can be seen, the regression line formula corresponding to each of the moisture contents applied to wheat samples is provided next to the legend of the previous figure.

Table 2 shows the mean \pm standard deviation results obtained for the angle of internal friction (ϕ) and the apparent cohesion (C) from the direct shear assays conducted with the different moisture contents selected.

Table 2. Mean \pm standard deviation for the angle of internal friction and the apparent cohesion the different moisture contents assayed.

Moisture Content (%) (d.b.)	Angle of Internal Friction (ϕ)	Apparent Cohesion (C, kPa)
7.5	22.9° \pm 0.6	10.98 \pm 1.82
10.0	24.9° \pm 0.5	10.37 \pm 1.59
10.5	24.6° \pm 0.6	12.50 \pm 1.88
13.4	24.8° \pm 0.3	9.62 \pm 1.01
15.5	28.6° \pm 0.5	6.47 \pm 1.88

From the above table, it can be seen that a moisture content of 15.5% returned the highest value for the angle of internal friction. Therefore, the greatest resistance to shearing was reached at the highest moisture content tested. As for the apparent cohesion, no great values were obtained in all cases, with this value decreasing as the moisture content increased.

When comparing the regression lines for the Mohr–Coulomb strength envelopes obtained at low (10, 20 and 50 kPa) and high normal stresses (100, 200 and 300 kPa), it could be observed that both curves intersect at one point at moisture contents of 7.5, 10.0 and 13.4%, as shown in Figure 8. Nevertheless, no intersection could be observed at normal stresses of 10.5 and 15.5%, as shown in Figure 9.

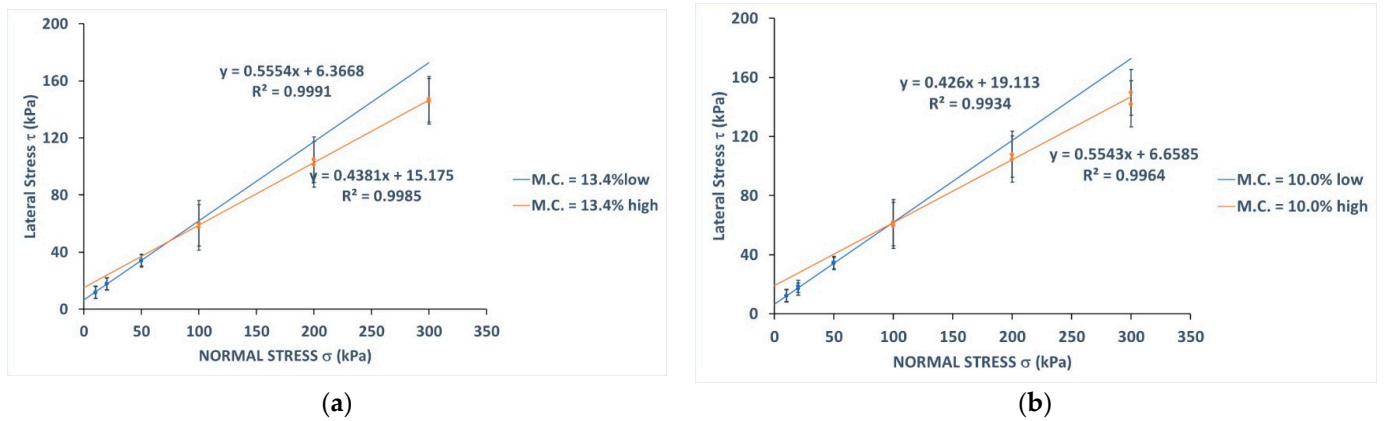


Figure 8. Regression lines for the Mohr–Coulomb strength envelopes obtained from direct shear assays conducted at low (10, 20 and 50 kPa) and high (100, 200 and 300 kPa) normal stresses and moisture contents of 13.4% (a) and 10.0% (b), respectively.

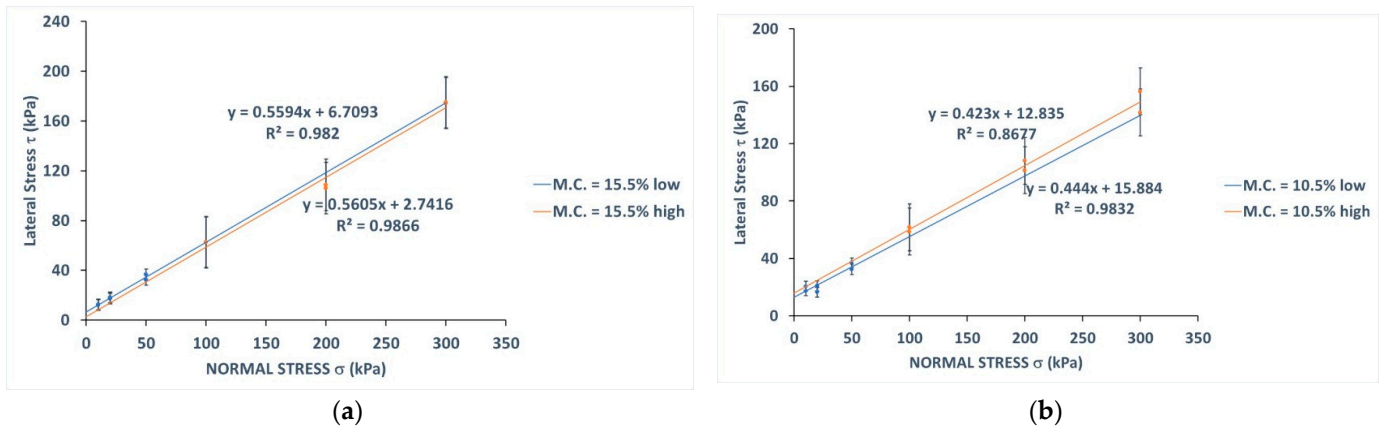


Figure 9. Regression lines for the Mohr–Coulomb strength envelopes obtained from direct shear assays conducted at low (10, 20 and 50 kPa) and high (100, 200 and 300 kPa) normal stresses and moisture contents of 15.5% (a) and 10.5% (b), respectively.

Obviously, the differences observed between the Mohr–Coulomb strength envelopes plotted in Figure 6 provided different values for the angle of internal friction and the apparent cohesion depending on the range of normal stresses applied (low or high). Table 3 shows the mean ± standard deviation for the internal angle of friction and the apparent cohesion at low and high normal stresses.

Table 3. Mean ± standard deviation for the internal angle of friction and the apparent cohesion the different moisture contents tested (d.b.) for ranges of low (10, 20 and 50 kPa) and high (100, 200 and 300 kPa) normal stresses.

Moisture Content (%) (d.b.)	Angle of Internal Friction (ϕ)		Apparent Cohesion (C, kPa)	
	Low Normal Stresses	High Normal Stresses	Low Normal Stresses	High Normal Stresses
7.5	28.2° ± 2.2	21.2° ± 1.1	6.81 ± 1.56	18.98 ± 4.88
10.0	29.0° ± 0.7	23.1° ± 0.8	6.66 ± 0.53	19.11 ± 3.76
10.5	22.9° ± 4.0	23.9° ± 1.4	12.83 ± 2.61	15.88 ± 6.26
13.4	29.0° ± 0.4	23.7° ± 0.4	6.37 ± 0.26	15.18 ± 1.81
15.5	29.2° ± 1.7	29.3° ± 1.4	6.71 ± 1.20	2.74 ± 7.06

With respect to the results obtained at low normal stresses, the tests conducted with the highest moisture content (15.5%) gave the greatest value for the internal angle of friction, whereas those conducted at the lowest moisture content (7.5%) provided the lowest value for this parameter. In any case, these values were of the same order at low normal stresses, with a difference of 3% between the extreme values obtained, except at 10.5% moisture content. The value obtained at 10.5% was significantly lower (21%) compared with that obtained at a moisture content of 10.0%. When analyzing the values obtained for this parameter when high normal stresses were applied, it could be observed that in general, the higher the moisture content of the samples, the higher the corresponding values for the internal angle of friction. Therefore, wheat samples offered greater resistance to shearing as moisture content increased. The only exception was the value recorded at 13.4%, which was similar to that obtained at a 10.5% moisture content.

As for the apparent cohesion values, those obtained at low normal stresses were lower than those recorded at high normal stresses. The only exception was the value obtained at high normal stresses at a moisture content of 15.5%, though in this case, the standard deviation could not be neglected.

3.2.2. Dilatancy Angle

Figure 10 shows the deformation curves obtained by direct shear assays at moisture contents of 13.4% (Figure 10a) and 7.5% (Figure 10b) under the different normal stresses applied (10, 20, 50, 100, 200 and 300 kPa). The vertical deformation (ε_V), needed for determining the dilatancy angle, is plotted on the ordinate axis, whereas the horizontal displacement (ε_H) is plotted on the abscissa. Each curve represents the mean values from the two repetitions.

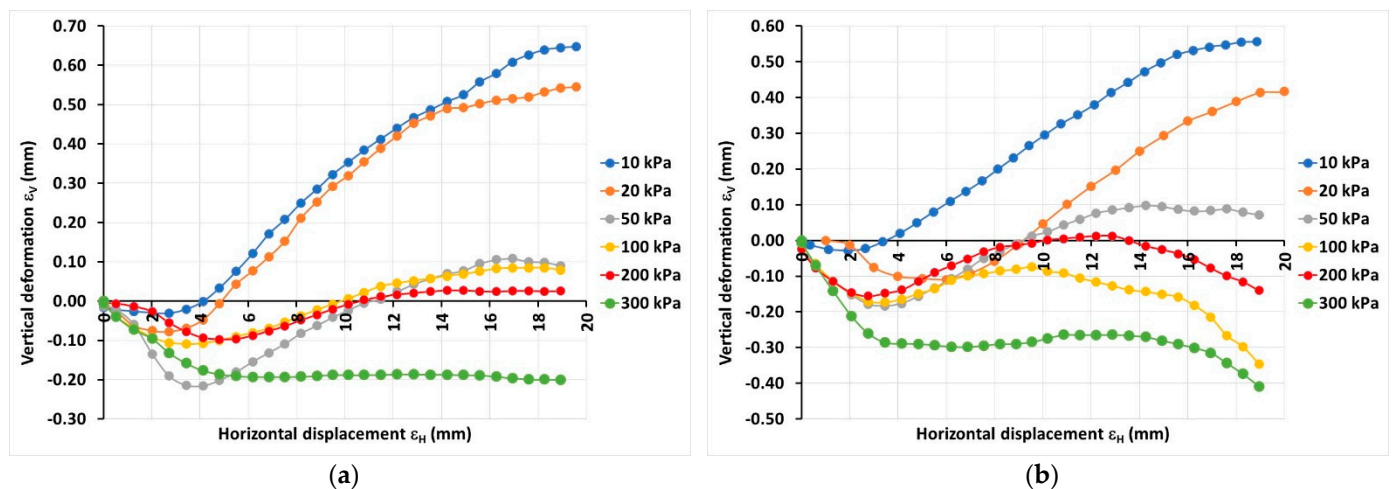


Figure 10. Deformation curves for wheat samples with (a) 13.4% moisture content and (b) 7.5% moisture content.

The different repetitions for each moisture content provided similar results. Immediately after beginning the assay, an initial compression of the samples took place as the particles adjusted their positions. The shearing stress was reached once the resistance they offered to shear was exceeded, then causing the displacement of the particles as they were less imbricated. This displacement increased the height of the vessel they occupied inside the shear box, depending on the normal stress applied in each case. Thus, for normal stresses up to 200 kPa, it was easy to observe this behavior. However, at the highest normal stress applied (300 kPa), it was not always possible to obtain a positive dilatancy since the thrust of the sample was not able to overcome that vertical stress. As expected, the vertical deformation values, and therefore the dilatancy angle values, were higher as when the applied normal stresses decreased because the particles were freer to move. This is

the reason why the difference in the vertical deformation recorded at 300 kPa and 10 kPa is significant.

Table 4 shows the mean \pm standard deviation for the dilatancy angles obtained under the different normal stresses tested.

Table 4. Mean \pm standard deviation for the dilatancy angle under the normal stresses assayed.

Normal Stress (kPa)	Dilatancy Angle (Ψ)				
	Moisture Content (d.b.)				
	7.5%	10.0%	10.5%	13.4%	15.5%
10	14.2° \pm 1.4	17.0° \pm 2.2	14.8° \pm 2.0	15.3° \pm 1.2	12.4° \pm 2.6
20	11.6° \pm 1.1	15.9° \pm 3.8	13.4° \pm 1.6	13.2° \pm 1.0	8.5° \pm 0.1
50	6.5° \pm 2.2	8.0° \pm 5.7	7.3° \pm 0.1	8.2° \pm 5.4	8.5° \pm 2.3
100	3.6° \pm 2.1	5.5° \pm 4.0	5.9° \pm 0.2	3.6° \pm 5.0	7.4° \pm 0.6
200	7.0° \pm 2.0	2.1° \pm 2.9	0.1° \pm 0.0	8.3° \pm 2.1	3.9° \pm 2.6
300	2.8° \pm 0.8	4.7° \pm 1.4	1.2° \pm 1.5	0.8° \pm 0.9	0.8° \pm 1.0

At lower normal stresses (10, 20 and 50 kPa), the assays conducted at a moisture content of 10.0% provided the highest dilatancy angles, with the maximum value (17.0°) recorded at 10 kPa. From these results, it was not possible to obtain a correlation between the values of this parameter and the moisture content applied to the samples. For the different moisture contents assayed, the dilatancy angle value fell as the normal stress exerted increased, though some exceptions occurred, such as that obtained at 10.0% and 10.5% moisture contents (4.7° and 1.2°, respectively) under a normal stress of 300 kPa, and that recorded at a 13.4% moisture content at a normal stress of 200 kPa (8.3°).

When analyzing the fall of the dilatancy angles, comparing the highest and the lowest values recorded for each moisture content assayed, the greatest percentage change was registered at a 10.5% moisture content (99%) between the minimum value (0.1°) and the maximum one (14.8°). This percentage change was 95% at 13.4% and 15.5% moisture contents, it achieved a value of 88% at a 10.0% moisture content and the smallest percentage change (80%) was registered at a 7.5% moisture content (the minimum value was 2.8° and the maximum was 14.2°).

3.3. Oedometric Assays

Figure 11 shows the curves obtained from the oedometric assays carried out for determining the change in apparent specific weight of the material when changing the normal stress applied. As shown below, the normal stress applied (σ) is plotted on the abscissa, whereas the apparent specific weight (γ) is plotted on the ordinate axis. In this type of assay, the moisture contents applied to wheat samples were the same as those selected for the direct shear tests, i.e., 7.5, 10.0, 10.5, 13.4% and 15.5% (d.b.), respectively.

The curves plotted on the previous figure correspond to the mean values obtained from the three repetitions carried out with wheat samples at each of the moisture contents applied. The general trend was that the higher the moisture content of the sample, the higher the value of the apparent specific weight recorded, except for the assays conducted at a moisture content of 15.5% since the corresponding curve is below that of 13.4%. As it was expected, in all cases, the peak value obtained for this parameter was achieved at the highest normal stress applied (256 kPa). Finally, during the unloading cycle, the slopes of the curves are quite similar, with a slight and progressive fall in the values of this parameter as the normal stress applied decreases, too. This trend was also followed but not as clearly for the remaining cases with a moisture content of 15.5%.

The curves plotted in Figure 12 show the change in apparent specific weight with the moisture content under the different normal stresses applied. The apparent specific weight is plotted on the ordinate axis, whereas the moisture content is plotted on the abscissa.

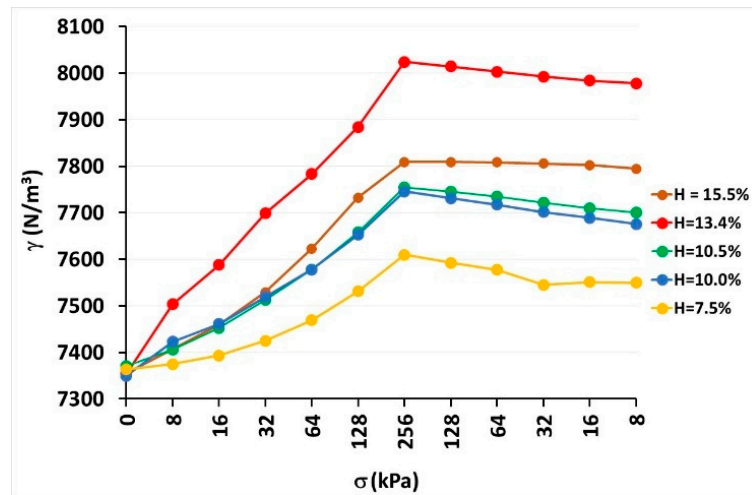


Figure 11. Variation in the apparent specific weight with the normal stress at different moisture contents.

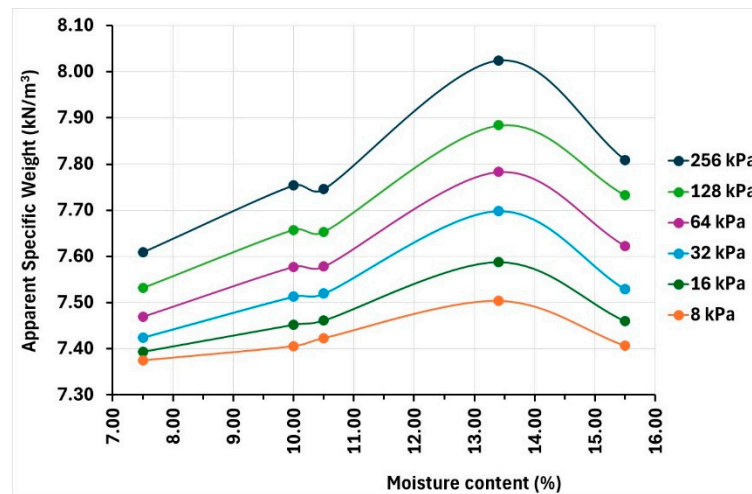


Figure 12. Variation in the apparent specific weight with the moisture content at different normal stresses applied.

The higher the normal stress applied to the samples, the higher the values of the apparent specific weight achieved. The shape of these curves is similar to that obtained in Proctor compaction tests with soils to determine the maximum density that a particular type of soil can be compacted to at an optimum water content.

Table 5 shows the mean ± standard deviation for the apparent specific weight values obtained under the different normal stresses and moisture contents tested.

Table 5. Mean ± standard deviation for the apparent specific weight under the normal stresses assayed.

Normal Stress (kPa)	Apparent Specific Weight (γ) (kN/m ³)				
	Moisture Content				
	7.5%	10.0%	10.5%	13.4%	15.5%
0	7.36 ± 0.00	7.37 ± 0.00	7.35 ± 0.00	7.35 ± 0.00	7.36 ± 0.00
8	7.38 ± 0.00	7.41 ± 0.02	7.42 ± 0.02	7.50 ± 0.01	7.41 ± 0.01
16	7.39 ± 0.01	7.45 ± 0.02	7.46 ± 0.02	7.59 ± 0.02	7.46 ± 0.01
32	7.43 ± 0.01	7.51 ± 0.03	7.52 ± 0.02	7.70 ± 0.02	7.53 ± 0.00
64	7.47 ± 0.01	7.58 ± 0.04	7.58 ± 0.02	7.78 ± 0.02	7.62 ± 0.02
128	7.53 ± 0.02	7.66 ± 0.04	7.65 ± 0.02	7.88 ± 0.02	7.73 ± 0.05
256	7.61 ± 0.04	7.75 ± 0.06	7.75 ± 0.02	8.02 ± 0.04	7.81 ± 0.06

Table 5. Cont.

Normal Stress (kPa)	Apparent Specific Weight (γ) (kN/m ³)				
	Moisture Content				
	7.5%	10.0%	10.5%	13.4%	15.5%
128	7.59 ± 0.03	7.75 ± 0.06	7.73 ± 0.02	8.01 ± 0.03	7.81 ± 0.06
64	7.58 ± 0.03	7.74 ± 0.06	7.72 ± 0.02	8.00 ± 0.02	7.81 ± 0.06
32	7.55 ± 0.01	7.72 ± 0.07	7.70 ± 0.02	7.99 ± 0.02	7.81 ± 0.06
16	7.55 ± 0.02	7.71 ± 0.07	7.69 ± 0.01	7.98 ± 0.01	7.80 ± 0.07
8	7.55 ± 0.02	7.70 ± 0.07	7.68 ± 0.01	7.98 ± 0.01	7.80 ± 0.07

Assays conducted at a moisture content of 13.4% provided the highest apparent specific weight, with values always close to 8.0 kN/m³. At this humidity, the apparent specific weight increased by some 9% at the highest normal stress compared to 0 kPa. However, this percentage fluctuated around 6% at a moisture content of 15.5%, around 5% at moisture contents of 10.0 and 10.5%, and around 3% at a moisture content of 7.5%.

4. Discussion

4.1. Moisture Content

The moisture contents selected in this work were within the range reported by other authors [13,37,52,53]. Therefore, the results provided from the assays conducted can be discussed with those found in the literature in cases where they exist.

4.2. Direct Shear Assays

4.2.1. Angle of Internal Friction and Apparent Cohesion

The shape of the curves obtained when the shear stress is plotted vs. the horizontal displacement is like those reported in previous works for other granular agricultural materials [20,23]. When comparing the results here obtained for the internal angle of friction with those reported by Moya et al. [23] under ambient humidity (9.76% moisture content) using the same material in both works, the minimum value recorded (22.9°) at a moisture content of 7.5% was 16% higher than that recorded in their work. In addition, this minimum value was up to 36% higher than that reported when triaxial assays were conducted at 10% axial deformation. However, the value provided for this parameter at a 10.0% moisture content (24.9°) was 3.7% higher than that recorded by these authors from direct shear assays (24.0°). In any case, the range of values overlap those reported by some authors, with values from 5% to 12% smaller [13,14,22,54], to around 10% to 16% higher [19–21]. Similar differences were found for the range of values obtained at low and high normal stress levels.

The differences might be attributed to differences in the moisture content, the arrangement of the particles, the bulk density, the orientation of the particles within the shear box, the formation of shear bands, the consolidation time (in some of those works cited, samples were previously consolidated) and the shape of the particles [13].

As mentioned, the wheat sample used in this work was the same assayed as Moya et al. [23] under ambient humidity. The values obtained for the apparent cohesion overlaps the range of values reported by these authors. On the other hand, the values here provided were notably higher than those reported in other works [13,19,20,22], considering that they ranged between 6.47 and 12.50 kPa, which were not too high values. Similar differences were found for the values obtained for this parameter at low normal stresses, whereas at high normal stresses, the maximum value (19.11 kPa) increased the difference with respect to those reported in the referred literature.

4.2.2. Dilatancy Angle

The range of dilatancy angle values are similar to those reported in the literature by some authors [19–23,55,56]. It was not possible to find within the literature information

related to the influence of moisture content on this parameter since all documents accessed referred to dry samples, i.e., under ambient humidity. The general trend showed that the dilatancy angle decreases as the normal stress increases, confirming the result stated by Zeng et al. [56].

4.3. Oedometric Assays

The apparent specific weight values ranged from 7.35 to 8.02 kN/m³, which correlate with those reported in numerous studies within the literature [14,15,17,20–23,37,57–59], although our result is 3% smaller than that reported in other works [60,61] and 6% higher than the minimum value provided in another one [13]. In this latter case, the values provided by the authors varied between 6.94 and 7.73 kN/m³, depending on the moisture content applied. In fact, that minimum value reported corresponded to a moisture content of 15.0%, whereas the values corresponding to moisture contents of 10.0% and 12.5% achieved 7.73 kN/m³ and 7.65 kN/m³, respectively, i.e., they were within the range of values here recorded from the assays conducted.

Higher apparent specific weight values were obtained as moisture content increased from 7.5 to 13.4%, then they decreased at a moisture content of 15.5%. This was not expected according to the results reported in some studies [52,62–64], which stated that bulk density decreased with an increase in moisture content. Moreover, some numerical models have been developed to predict the decrease in bulk density as moisture content increased [53,65]. These studies consider that wheat is more compressible at higher moisture contents than at lower moisture contents [66]. Despite this, some studies have reported values of bulk density to be moisture-dependent, showing a similar tendency to that provided in this work, with values increasing up to a moisture content of 13.3% and decreasing at higher moisture contents [37], and with values at 17.5 and 20.0% moisture contents higher than those obtained at a 15% moisture content [13]. Maybe the presence of water could affect the orientation and the arrangement of the particles in the oedometer cells.

The values here provided, considering the influence of moisture content on some mechanical properties of wheat, can be useful for wheat handling and storage. In addition, since these properties of granular solids depend on many factors such as storage moisture, temperature, relative humidity, etc., they play a significant role in their resulting storage and flow behavior [36,67–76]. Therefore, similar studies should be conducted with other granular materials to design appropriate, efficient and economic handling and storage equipment and structures for bulk solids [67].

5. Conclusions

From the direct shear assays, it could be confirmed that the values of the internal angle of friction correlated with those reported in the literature. Nevertheless, the apparent cohesion values obtained here were not too high, although they were mostly higher than those found in the literature.

The range of dilatancy angle values were within the ranges reported in the literature. It could be confirmed that as a general trend, the values of this parameter decreased as the normal stress applied increased.

In general, the apparent specific weight values recorded were similar or very close to those reported in the literature. The values of this parameter increased up to a moisture content of 13.4%, then decreased at higher moisture contents. This trend was inconsistent with what was observed and modeled in other works, although it coincided with what was published in some other works.

The values here provided for wheat can be useful to model and design appropriate, efficient and economic handling and storage structures and equipment for bulk solids.

Author Contributions: Conceptualization, M.M.; methodology, M.M. and J.R.V.-G.; software, M.M.; validation, M.M., J.R.V.-G., D.S. and J.Á.R.; formal analysis, M.M., D.S. and J.Á.R.; investigation, M.M., J.R.V.-G., D.S. and J.Á.R.; data curation, M.M., D.S. and J.Á.R.; writing—original draft preparation, M.M.; writing—review and editing, M.M., J.R.V.-G., D.S. and J.Á.R.; supervision, M.M., J.R.V.-G., D.S.

and J.Á.R.; funding acquisition, M.M. and J.R.V.-G. All authors have read and agreed to the published version of the manuscript.

Funding: This research and APC was funded by the Spanish “Agencia Estatal de Investigación” via the research project “Study of the structural behavior of corrugated wall silos using Discrete Element Models (SILODEM)”, grant number PID2019-107051GB-I00/AEI/10.13039/501100011033.

Data Availability Statement: The original contributions presented in the study are included in the article, further inquiries can be directed to the corresponding author/s.

Acknowledgments: The authors thank Leonesa Astur de Piensos, S.A. (LESA) company for providing the wheat used in this research.

Conflicts of Interest: The authors declare no conflict of interest. The funders had no role in the design of the study; in the collection, analyses, or interpretation of data; in the writing of the manuscript, or in the decision to publish the results.

References

- Janssen, H. Versuche Über Getreidebruck in Silozellen. *Z. Vereines Dtsch. Ingenieure* **1895**, *39*, 1045–1049.
- Jofriet, J.C.; Lelievre, B.; Fwa, T.F. Friction Model for Finite Element Analyses of Silos. *Trans. Am. Soc. Agric. Eng.* **1977**, *20*, 735–740. [[CrossRef](#)]
- Ayuga, F.; Guaita, M.; Aguado, P. Static and Dynamic Silo Loads Using Finite Element Models. *J. Agric. Eng. Res.* **2001**, *78*, 299–308. [[CrossRef](#)]
- Patwa, A.; Ambrose, R.P.K.; Casada, M.E. Discrete Element Method as an Approach to Model the Wheat Milling Process. *Powder Technol.* **2016**, *302*, 350–356. [[CrossRef](#)]
- Ai, J.; Chen, J.F.; Rotter, J.M.; Ooi, J.Y. Finite Element Prediction of Progressively Formed Conical Stockpiles. In Proceedings of the Simulia Customer Conference 2009, London, UK, 18–21 May 2009; pp. 1–13.
- Wang, Y.; Lu, Y.; Ooi, J.Y. A Numerical Study of Wall Pressure and Granular Flow in a Flat-Bottomed Silo. *Powder Technol.* **2015**, *282*, 43–54. [[CrossRef](#)]
- Rotter, J.M.; Holst, J.M.F.G.; Ooi, J.Y.; Sanad, A.M. Silo Pressure Predictions Using Discrete-Element and Finite-Element Analyses. *Philos. Trans. R. Soc. A Math. Phys. Eng. Sci.* **1998**, *356*, 2685–2712. [[CrossRef](#)]
- Kobyłka, R.; Molenda, M.; Horabik, J. Loads on Grain Silo Insert Discs, Cones, and Cylinders: Experiment and DEM Analysis. *Powder Technol.* **2019**, *343*, 521–532. [[CrossRef](#)]
- Madrid, M.A.; Fuentes, J.M.; Ayuga, F.; Gallego, E. Determination of the Angle of Repose and Coefficient of Rolling Friction for Wood Pellets. *Agronomy* **2022**, *12*, 424. [[CrossRef](#)]
- González-Montellano, C.; Gallego, E.; Ramírez-Gómez, Á.; Ayuga, F. Three Dimensional Discrete Element Models for Simulating the Filling and Emptying of Silos: Analysis of Numerical Results. *Comput. Chem. Eng.* **2012**, *40*, 22–32. [[CrossRef](#)]
- Briassoulis, D. Finite Element Analysis of a Cylindrical Silo Shell under Unsymmetrical Pressure Distributions. *Comput. Struct.* **2000**, *78*, 271–281. [[CrossRef](#)]
- Horabik, J.; Parafiniuk, P.; Molenda, M. Stress Profile in Bulk of Seeds in a Shallow Model Silo as Influenced by Mobilisation of Particle-Particle and Particle-Wall Friction: Experiments and DEM Simulations. *Powder Technol.* **2018**, *327*, 320–334. [[CrossRef](#)]
- Molenda, M.; Horabik, J. *Mechanical Properties of Granular Agro-Materials and Food Powders for Industrial Practice. Part I: Characterization of Mechanical Properties of Particulate Solids for Storage and Handling*; Horabik, J., Laskowski, J., Eds.; Institute of Agrophysics Polish Academy of Science: Lublin, Poland, 2005.
- Lebègue, Y.; Boudakian, A. Bases Des Règles «Silos» Du SNBATI—Essais Sur Les Produits et Principes Des Formules «Silos». *Ann. ITBTP* **1989**, *476*, 69–113.
- Bucklin, R.A.; Molenda, M.; Bridges, T.C.; Ross, I.J. Slip-Stick Frictional Behavior of Wheat on Galvanized Steel. *Trans. Am. Soc. Agric. Eng.* **1996**, *39*, 649–653. [[CrossRef](#)]
- Bucklin, R.A.; Thompson, S.A.; Ross, I.J.; Biggs, R.H. Apparent Dynamic Coefficient of Friction of Corn on Galvanized Steel Bin Wall Material. *Trans. Am. Soc. Agric. Eng.* **1993**, *36*, 1915–1918. [[CrossRef](#)]
- Thompson, S.A.; Bucklin, R.A.; Batich, C.D.; Ross, I.J. Variation in the Apparent Coefficient of Friction of Wheat on Galvanized Steel. *Trans. ASAE* **1988**, *31*, 1518–1524. [[CrossRef](#)]
- Ramírez, A.; Moya, M.; Ayuga, F. Determination of the Mechanical Properties of Powdered Agricultural Products and Sugar. *Part. Part. Syst. Charact.* **2010**, *26*, 220–230. [[CrossRef](#)]
- Molenda, M.; Stasiak, M.; Moya, M.; Ramirez, A.; Horabik, J.; Ayuga, F. Testing Mechanical Properties of Food Powders in Two Laboratories-Degree of Consistency of Results. *Int. Agrophys.* **2006**, *20*, 37–45.
- Moya, M.; Aguado, P.J.; Ayuga, F. Mechanical Properties of Some Granular Agricultural Materials Used in Silo Design. *Int. Agrophys.* **2013**, *27*, 181–193. [[CrossRef](#)]
- Moya, M.; Ayuga, F.; Guaita, M.; Aguado, P.J. Mechanical Properties of Granular Agricultural Materials. *Trans. ASAE* **2002**, *45*, 1569–1577. [[CrossRef](#)]

22. Moya, M.; Guaita, M.; Aguado, P.; Ayuga, F. Mechanical Properties of Granular Agricultural Materials, Part 2. *Trans. ASABE* **2006**, *49*, 479–489. [[CrossRef](#)]
23. Moya, M.; Sánchez, D.; Villar-García, J.R. Values for the Mechanical Properties of Wheat, Maize and Wood Pellets for Use in Silo Load Calculations Involving Numerical Methods. *Agronomy* **2022**, *12*, 1261. [[CrossRef](#)]
24. Wójcik, A.; Frączek, J. The Methodical Aspects of the Friction Modeling of Plant Granular Materials. *Powder Technol.* **2019**, *344*, 504–513. [[CrossRef](#)]
25. Wójcik, A.; Frączek, J. The Problem of Standardising the Static Friction Force Measurement in Plant Granular Materials. *Powder Technol.* **2022**, *398*, 117133. [[CrossRef](#)]
26. Wójcik, A.; Frączek, J.; Niemczewska-Wójcik, M. Methodological Problems of Friction Force Measurement of Plant Granular Materials. *Tribol. Int.* **2023**, *188*, 108886. [[CrossRef](#)]
27. Kibar, H.; Öztürk, T.; Esen, B. The Effect of Moisture Content on Physical and Mechanical Properties of Rice (*Oryza sativa* L.). *Span. J. Agric. Res.* **2010**, *8*, 741–749. [[CrossRef](#)]
28. Mattsson, J.E.; Kofman, P.D. Influence of Particle Size and Moisture Content on Tendency to Bridge in Biofuels Made from Willow Shoots. *Biomass Bioenergy* **2003**, *24*, 429–435. [[CrossRef](#)]
29. Ponce-García, N.; Ramírez-Wong, B.; Torres-Chávez, P.I.; De Dios Figueroa-Cárdenas, J.; Serna-Saldívar, S.O.; Cortez-Rocha, M.O. Effect of Moisture Content on the Viscoelastic Properties of Individual Wheat Kernels Evaluated by the Uniaxial Compression Test under Small Strain. *Cereal Chem.* **2013**, *90*, 558–563. [[CrossRef](#)]
30. Brar, H.S.; Sidhu, G.K.; Singh, A. Effect of Moisture Content on Engineering Properties of Oats (*Avena sativa* L.). *Agric. Eng. Int. CIGR J.* **2016**, *18*, 186–193.
31. Zaalouk, A.K.; Zabady, F.I. Effect of Moisture Content on Angle of Repose and Friction Coefficient of Wheat Grain. *Misr J. Agric. Eng.* **2009**, *26*, 418–427. [[CrossRef](#)]
32. Davies, R.M.; El-Okene, A.M. Moisture-Dependent Physical Properties of Soybeans. *Int. Agrophys.* **2009**, *23*, 299–303.
33. Lancaster, J.K. A Review of the Influence of Environmental Humidity and Water on Friction, Lubrication and Wear. *Tribol. Int.* **1990**, *23*, 371–389. [[CrossRef](#)]
34. Wiacek, J.; Molenda, M. Moisture-Dependent Physical Properties of Rapeseed-Experimental and DEM Modeling. *Int. Agrophys.* **2011**, *25*, 59–65.
35. Wandkar, S.V.; Ukey, P.D.; Pawar, D.A. Determination of Physical Properties of Soybean at Different Moisture Levels. *Agric. Eng. Int. CIGR J.* **2012**, *14*, 138–142.
36. Teunou, E.; Fitzpatrick, J.J. Effect of Relative Humidity and Temperature on Food Powder Flowability. *J. Food Eng.* **1999**, *42*, 109–116. [[CrossRef](#)]
37. Cheng, X.; Zhang, Q.; Shi, C.; Yan, X. Model for the Prediction of Grain Density and Pressure Distribution in Hopper-Bottom Silos. *Biosyst. Eng.* **2017**, *163*, 159–166. [[CrossRef](#)]
38. Gorji, A.; Rajabipour, A.; Tavakoli, H. Fracture Resistance of Wheat Grain as a Function of Moisture Content, Loading Rate and Grain Orientation. *Aust. J. Crop Sci.* **2010**, *4*, 448–452.
39. Landi, G.; Barletta, D.; Poletto, M. Modelling and Experiments on the Effect of Air Humidity on the Flow Properties of Glass Powders. *Powder Technol.* **2011**, *207*, 437–443. [[CrossRef](#)]
40. Louati, H.; Oulahna, D.; de Ryck, A. Effect of the Particle Size and the Liquid Content on the Shear Behaviour of Wet Granular Material. *Powder Technol.* **2017**, *315*, 398–409. [[CrossRef](#)]
41. Frye, K.M.; Marone, C. Effect of Humidity on Granular Friction at Room Temperature. *J. Geophys. Res. Solid. Earth* **2002**, *107*, ETG 11-1–ETG 11-13. [[CrossRef](#)]
42. Nokhodchi, A. An Overview of the Effect of Moisture on Compaction and Compression. *Pharm. Technol.* **2005**, *29*, 46–66.
43. Delenne, J.Y.; Soulié, F.; El Youssofi, M.S.; Radjai, F. From Liquid to Solid Bonding in Cohesive Granular Media. *Mech. Mater.* **2011**, *43*, 529–537. [[CrossRef](#)]
44. Delenne, J.; El Youssofi, M.; Cherblanc, F.; Béné, J. Mechanical Behavior and Failure of Cohesive Granular Materials. *Int. J. Numer. Anal. Methods Geomech.* **2004**, *28*, 1577–1594. [[CrossRef](#)]
45. Jiang, M.J.; Yu, H.S.; Harris, D. Bond Rolling Resistance and Its Effect on Yielding of Bonded Granulates by DEM Analyses. *Int. J. Numer. Anal. Methods Geomech.* **2006**, *30*, 723–761. [[CrossRef](#)]
46. Louati, H.; Oulahna, D.; de Ryck, A. Apparent Friction and Cohesion of a Partially Wet Granular Material in Steady-State Shear. *Powder Technol.* **2015**, *278*, 65–71. [[CrossRef](#)]
47. Richefeu, V.; El Youssofi, M.S.; Radjai, F. Shear Strength of Unsaturated Soils: Experiments, DEM Simulations, and Micromechanical Analysis. In *Theoretical and Numerical Unsaturated Soil Mechanics*; Springer: Berlin/Heidelberg, Germany, 2007; pp. 83–91.
48. Richefeu, V.; El Youssofi, M.S.; Radjai, F. Shear Strength Properties of Wet Granular Materials. *Phys. Rev. E Stat. Nonlin Soft Matter Phys.* **2006**, *73*, 051304. [[CrossRef](#)]
49. UNE-EN ISO 17892-1; Geotechnical Investigation and Testing. Laboratory Testing of Soil. Part 1: Determination of Water Content. AENOR: Madrid, Spain, 2015.
50. UNE-EN ISO 17892-10; Geotechnical Investigation and Testing. Laboratory Testing of Soil. Part 10: Direct Shear Tests. AENOR: Madrid, Spain, 2018.
51. UNE-EN ISO 17892-5; Geotechnical Investigation and Testing. Laboratory Testing of Soil. Part 5: Incremental Loading Oedometer Test. AENOR: Madrid, Spain, 2017.

52. Tabatabaefar, A. Moisture-Dependent Physical Properties of Wheat. *Int. Agrophys.* **2003**, *17*, 207–211.
53. Gao, M.; Cheng, X.; Du, X. Simulation of Bulk Density Distribution of Wheat in Silos by Finite Element Analysis. *J. Stored Prod. Res.* **2018**, *77*, 1–8. [[CrossRef](#)]
54. Moysey, E.; Lambert, E.; Wang, Z. Flow Rates of Grains and Oilseeds through Sharp-Edged Orifices. *Trans. Am. Soc. Agric. Eng.* **1988**, *31*, 226–231. [[CrossRef](#)]
55. Zeng, C.; Wang, Y. The Shear Strength and Dilatancy Behavior of Wheat Stored in Silos. *Complexity* **2019**, *2019*, 1547616. [[CrossRef](#)]
56. Zeng, C.; Gu, H.; Wang, Y. Stress-Strain Response of Sheared Wheat Granular Material Stored in Silos Using Triaxial Compression Tests. *Int. Agrophys.* **2020**, *34*, 103–114. [[CrossRef](#)]
57. Zhang, Q.; Britton, M.G. A Micromechanics Model for Predicting Dynamic Loads during Discharge in Bulk Solids Storage Structures. *Can. Biosyst. Eng./Le Genie Des Biosyst. Au Can.* **2003**, *45*, 5.21–5.27.
58. Zhang, Q.; Li, Y.; Puri, V.M.; Manbeck, H.B. Physical Properties Effect on Stress-Strain Behavior of Wheat En Masse-Part II. Constitutive Elastoplastic Parameter Dependence on Initial Bulk Density and Moisture Content. *Trans. Am. Soc. Agric. Eng.* **1989**, *32*, 203–209. [[CrossRef](#)]
59. Reimbert, M.; Reimbert, A. *Silos. Theory and Practice*; Lavoisier: Paris, France, 1987; ISBN 9782852063655.
60. Zeng, C.; Wang, Y. Compressive Behaviour of Wheat from Confined Uniaxial Compression Tests. *Int. Agrophys.* **2019**, *33*, 347–354. [[CrossRef](#)] [[PubMed](#)]
61. Sinha, R.N.; Muir, W.E. *Grain Storage: Part of a System*; Sinha, R.N., Muir, W.E., Eds.; Avi Publishing Company: Madison, WI, USA, 1973.
62. Carman, K. Some Physical Properties of Lentil Seeds. *J. Agric. Engng Res.* **1996**, *63*, 87–92. [[CrossRef](#)]
63. Dutta, S.K.; Nema, V.K.; Bhardwaj, R.K. Physical Properties of Gram. *J. Agric. Eng. Res.* **1988**, *39*, 259–268. [[CrossRef](#)]
64. Shepherd, H.; Bhardwaj, R.K. Moisture-Dependent Physical Properties of Pigeon Pea. *J. Agric. Eng. Res.* **1986**, *35*, 227–234. [[CrossRef](#)]
65. Turner, A.P.; Montross, M.D.; McNeill, S.G.; Sama, M.P.; Casada, M.C.; Boac, J.M.; Bhadra, R.E.; Maghirang, R.G.; Thompson, S.A. Modeling the Compressibility Behavior of Hard Red Wheat Varieties. *Trans. ASABE* **2016**, *59*, 1029–1038.
66. Thompson, S.A.; Ross, I.J. Compressibility and Frictional Coefficients of Wheat. *Trans. ASAE* **1983**, *26*, 1171–1176. [[CrossRef](#)]
67. Ganesan, V.; Rosentrater, K.A.; Muthukumarappan, K. Flowability and Handling Characteristics of Bulk Solids and Powders—A Review with Implications for DDGS. *Biosyst. Eng.* **2008**, *101*, 425–435. [[CrossRef](#)]
68. Zhang, S.; Lin, P.; Wang, C.L.; Tian, Y.; Wan, J.F.; Yang, L. Investigating the Influence of Wall Frictions on Hopper Flows. *Granul. Matter* **2014**, *16*, 857–866. [[CrossRef](#)]
69. Lanzerstorfer, C.; Hinterberger, M. Influence of the Moisture Content on the Flowability of Fine-Grained Iron Ore Concentrate. *Int. J. Chem. Mol. Eng.* **2017**, *11*, 265–268.
70. Capece, M.; Silva, K.R.; Sunkara, D.; Strong, J.; Gao, P. On the Relationship of Inter-Particle Cohesiveness and Bulk Powder Behavior: Flowability of Pharmaceutical Powders. *Int. J. Pharm.* **2016**, *511*, 178–189. [[CrossRef](#)] [[PubMed](#)]
71. Bian, Q.; Sittipod, S.; Garg, A.; Ambrose, R.P.K. Bulk Flow Properties of Hard and Soft Wheat Flours. *J. Cereal Sci.* **2015**, *63*, 88–94. [[CrossRef](#)]
72. Mellmann, J.; Hoffmann, T.; Füll, C. Mass Flow during Unloading of Agricultural Bulk Materials from Silos Depending on Particle Form, Flow Properties and Geometry of the Discharge Opening. *Powder Technol.* **2014**, *253*, 46–52. [[CrossRef](#)]
73. Tomasetta, I.; Barletta, D.; Poletto, M. Correlation of Powder Flow Properties to Interparticle Interactions at Ambient and High Temperatures. *Particuology* **2014**, *12*, 90–99. [[CrossRef](#)]
74. Littlefield, B.; Fasina, O.O.; Shaw, J.; Adhikari, S.; Via, B. Physical and Flow Properties of Pecan Shells-Particle Size and Moisture Effects. *Powder Technol.* **2011**, *212*, 173–180. [[CrossRef](#)]
75. González-Montellano, C.; Ayuga, F.; Ooi, J.Y. Discrete Element Modelling of Grain Flow in a Planar Silo: Influence of Simulation Parameters. *Granul. Matter* **2011**, *13*, 149–158. [[CrossRef](#)]
76. Couto, A.; Ruiz, A.; Aguado, P.J. Experimental Study of the Pressures Exerted by Wheat Stored in Slender Cylindrical Silos, Varying the Flow Rate of Material during Discharge. Comparison with Eurocode 1 Part 4. *Powder Technol.* **2013**, *237*, 450–467. [[CrossRef](#)]

Disclaimer/Publisher’s Note: The statements, opinions and data contained in all publications are solely those of the individual author(s) and contributor(s) and not of MDPI and/or the editor(s). MDPI and/or the editor(s) disclaim responsibility for any injury to people or property resulting from any ideas, methods, instructions or products referred to in the content.